is to increase the turbulent mixing in the separated shear layer, thus increasing the separation shear flow thickness and the rate of entrainment of fluid from the wake. This results in greater streamline curvature around the prism and a decrease in radius of curvature of the shear layer. Increasing turbulence intensity thus results in earlier reattachment when compared with a similar flow situation with lower turbulence intensity. As the front wall face does not involve separation streamlines, it is thus not significantly affected by a higher turbulence intensity. This is evident from the average $C_{p,\text{mean}}$ values at each level on the front face as shown in Fig. 3. For the sides immersed in the wake, however, the average $C_{p,\text{mean}}$ values become markedly more negative in magnitude at higher turbulence intensities. The results do not show a pressure recovery that would imply a reattachment of flow. The absence of the pressure recovery on the leeward side of the prism is probably due to the sharp corners and short breadth of the prism.

Conclusions

Through this limited investigation, it was found that, for approaching uniform flow with various approaching turbulence intensities in the range of 05–30%, the effects of the free end of a triangular prism are limited to a region $<1d$ from the free end on the front face of the prism. On the faces immersed in the wake region, the end effects are limited to the region $<3d$ from the free end. The pressure coefficients on the surface facing the approaching flow do not appear to be significantly affected by the range of turbulence intensities investigated. For the sides immersed in the wake of the separation streamlines from the leading edges, the $C_{p,\text{mean}}$ values become markedly more negative in magnitude at higher turbulence intensities.

References

[1]El-Sherbiny, S., "Flow Separation and Reattachment over the Side of a 90 deg Triangular Prism," *Journal of Wind Engineering and Industrial Aerodynamics*, Vol. 11, 1983, pp. 393–403.

[2]Twigge-Molecey, C. F. M., and Baines, W. D., "Aerodynamic Forces on a Triangular Cylinder," *ASCE, Journal of the Engineering Mechanics Division*, Vol. 99, 1973, pp. 803–818.

Experimental Investigation of Velocity Slip near an Arcjet Exit Plane

J. G. Liebeskind,* R. K. Hanson,† and M. A. Cappelli‡
Stanford University, Stanford, California 94305

Introduction

VELOCITY slip is a phenomenon associated with multicomponent flows in which species of different mass have different mean velocities. This phenomenon has been studied in molecular beam nozzles[1] and has been exploited for isotope separation.[2] Significant velocity slip has been measured in the plume of low-power arcjet thrusters.[3] These recent measurements, obtained by mass spectrometry of a molecular beam sampling probe, were limited to locations more than 10 diameters from the exit plane.

The determination of whether slip develops in the nozzle, near the exit plane, or in the expansion plume of an arcjet thruster, is important to both modeling efforts and to the interpretation of measurements. If velocity slip develops inside the nozzle, numerical models will need to include separate momentum equations for each neutral species or, at the very least, an appropriate model for multicomponent transport. These additions increase the complexity of an already difficult task. Measurements of exit-plane velocity in these devices have recently been made by laser-induced fluorescence (LIF),[4] a species specific technique. If significant velocity slip exists, then separate measurements for each species are necessary to completely characterize the flowfield.

We have previously reported LIF-based measurements of atomic hydrogen velocity and kinetic temperature in a hydrogen-fueled arcjet.[4,5] We recognize, however, that the flow consists of both atomic and molecular hydrogen (along with small fractions of ions and electrons). The most direct method to investigate velocity slip in the arcjet flowfield would be to measure, in addition to the velocity of atomic hydrogen, the velocity of molecular hydrogen under the same conditions. As with atomic hydrogen, absorption transitions from the ground state require vacuum-ultraviolet wavelengths. Owing to the low densities of excited-state molecules and the rovibrational distribution which reduces the density of any particular state, these transitions are difficult to probe.

A simpler approach, for the purpose of evaluating slip, is to seed the flow with a species that is accessible with the same laser used to probe atomic hydrogen. In the present study, helium was chosen as the seed species owing to its inertness (with respect to the arcjet nozzle), its relative mass (four times the mass of atomic hydrogen), and its convenient electronic transitions in the visible wavelength region. Velocity and temperature are measured by LIF of both helium and atomic hydrogen at the same arcjet operating condition. Absence of slip between helium and atomic hydrogen would suggest that slip is not a dominant mechanism in the nozzle or exit plane vicinity of our hydrogen arcjet.

Theory

In a multicomponent mixture, each species (denoted by i), may have its own mean velocity v_i, and the mean mass velocity v_m is defined by

$$v_m = \frac{\sum n_i m_i v_i}{\sum n_i m_i} \tag{1}$$

Here, n_i is the number density of species i and m_i is the mass. The simplified steady-state momentum equation for a single species in the axial direction z can be expressed as

$$n_i m_i v_i \frac{\partial v_i}{\partial z} + \frac{\partial p_i}{\partial z} = n_i m_i \sum_j k_{ij}(v_j - v_i) \tag{2}$$

where p_i is the partial pressure. The term on the right side of Eq. (2) represents the momentum exchange between species of different types due to collisions. The momentum exchange term formulated in this way assumes that the force per unit volume exerted on particles of species i, due to collisions with species of type j, is proportional to the difference between their respective mean velocities. The proportionality constant k_{ij}, which accounts for differences in mass of the colliding particles, can be considered a collision frequency for momentum transfer. This constant can be determined from kinetic theory.[6,7] The slip velocity v_{slip} is usually defined for a binary mixture as the difference in velocities,

$$v_{\text{slip}} = v_j - v_i \tag{3}$$

If the density is high such that flow is in a continuum regime, the collision rate will be high, allowing efficient momentum exchange between species. Thus, the different species will be in equilibrium, and the slip velocity will be negligible. However, in an expanding flow, conditions can occur in the transition from continuum to free molecular flow, where velocity and pressure gradients are large and the collision rates are low. Insufficient collisions for momentum exchange between species allows a slip velocity to develop. The

Received March 12, 1994; revision received Aug, 10, 1994; accepted for publication Aug. 19, 1994. Copyright © 1994 by the authors. Published by the American Institute of Aeronautics and Astronautics, Inc., with permission.

*Research Assistant, High Temperature Gasdynamics Laboratory, Department of Mechanical Engineering. Student Member AIAA.

†Chairman, High Temperature Gasdynamics Laboratory, Department of Mechanical Engineering. Associate Fellow AIAA.

‡Assistant Professor, High Temperature Gasdynamics Laboratory, Department of Mechanical Engineering. Member AIAA.

proportionality constant k_{ij} is inversely proportional to the Knudsen number Kn (Ref. 7)

$$k_{ij} \propto 1/Kn \tag{4}$$

As the Knudsen number increases within the continuum regime, momentum transfer between species decreases. However, as the flow becomes rarefied to the extent that collisions become negligible, the slip approaches a constant value (which may be zero) and Eq. (2) is no longer valid. The Knudsen number for this flow has been determined, based on experimental results, to be just under unity.[5] This puts the flow regime in the transition between continuum and rarefied flow.

Experiment

The arcjet thruster used in this experiment is a 1-kW class radiatively cooled thruster designed and built at NASA Lewis Research Center. The tungsten nozzle has a 0.64-mm-diam throat, 0.25-mm-long constrictor, and a conical (20-deg half-angle) diverging section with an area ratio of 225 (9.53-mm exit diameter). A more complete description of the arcjet is available elsewhere.[8,9] When operating on the hydrogen-helium mixture, the current and voltage are 9.5 A and 143 V corresponding to 1.36 kW arc power. The arcjet is operated in a 0.56-m-diam cylindrical stainless steel chamber 1.09 m long. The 0.5-Torr background pressure is maintained by two 35.4 m^3/min coupled to the chamber with 152-mm-diam pipe.

The temperature and velocity measurements were made using LIF. A continuous wave ring dye laser scans across the atomic transition. Since the laser bandwidth is much smaller than the spectral feature, the fluorescence excitation spectrum accurately depicts the broadening mechanisms of the probed species. The velocity is determined from the Doppler shift whereas the temperature is inferred from the shape of the fluorescence excitation spectrum using a Doppler-broadened line-shape model.[4] Since Doppler broadening arises from the velocity distribution of the species, this diagnostic technique probes the kinetic or translational temperature which may differ from the electronic, rotational, and vibrational temperatures of the molecular species in the flow.[10,11] Details of the implementation and analysis have been published previously[4]; the only difference in this experiment is the use of optogalvanic detection in a dc discharge for the helium reference (unshifted) signal. The optogalvanic cell provided a reference for helium with a high signal-to-noise ratio. Fluorescence and absorption in a microwave discharge were used for a hydrogen reference calibration because it provided a stronger signal-to-noise ratio than the optogalvanic technique.

The atomic hydrogen transition probed is the Balmer α transition at 656 nm (15,233 cm^{-1}), an electronic transition between the first and second excited states of H, i.e., $n = 2 \rightarrow n = 3$. This transition actually consists of the overlap of several fine structure components. Since the separation of these components is of the same magnitude as the broadening, the fine structure must be accounted for when analyzing the line shape. The helium transition probed is the $2^1P \rightarrow 3^1D$ transition at 668 nm (14,970 cm^{-1}).

The relatively high energy of helium's first excited state, 166,278 cm^{-1} (20.6 eV) above the ground state can lead to weak fluorescence signals. To obtain a significantly strong fluorescence signal (relative to the noise), a high helium flow rate of 6.2 standard liters/min (SLPM) was necessary. This is significant when compared to the 9.0 SLPM of hydrogen, and hence altered the normal operating conditions of the arcjet. In particular, the addition of helium to the propellant increases the arc voltage and reduces the velocities. The voltage increase of less than 3 V can be explained by a combination of the increased mass flow (due to the helium addition) and helium's higher ionization energy. The 30% velocity decrease (at the centerline) can be attributed to helium's higher atomic mass and the reduced specific power. Also, the peak temperature drops 20% from 5000 K to 4000 K. Although the addition of the helium modifies the flow parameters, the conditions that may lead to slip are expected to be similar to those encountered in the unseeded g arcjet.

Results and Conclusions

The raw data from the helium and hydrogen fluorescence are shown in Figs. 1 and 2, respectively. The Doppler shifts correspond to axial velocities of 10.4 km/s for helium and 10.3 km/s for hydrogen. The magnitude of these measurements is consistent with previous measurements,[4,5] thrust measurements,[8] and model predictions.[12] The hydrogen and helium velocities agree within the 0.2 km/s uncertainty of the measurement. This indicates that the slip velocity is less than the uncertainty of the measurement; i.e., the upper limit of the slip velocity is about 2% of either species' velocity.

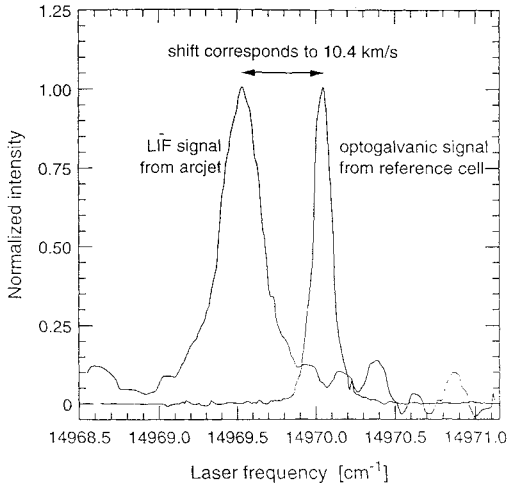

Fig. 1 Doppler-shifted fluorescence excitation spectrum of helium along with the unshifted reference signal used to calibrate the wave meter, probe volume centered in the plume, 0.5 mm from the exit plane.

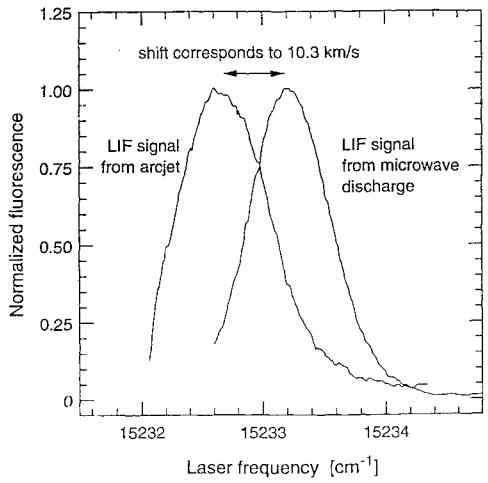

Fig. 2 Doppler shift of atomic hydrogen measured relative to its calibration, measurement location same as the helium data; note the smaller atomic mass leads to broader line widths even though the temperature is the same.

The inferred temperature for helium and hydrogen are 3990 K and 4260 K, respectively. The 6% difference is less than the 20% uncertainty of the measurement. These results allow us to conclude that all species share a common kinetic temperature. Because of the higher sensitivity to noise, the uncertainties of the temperature are higher than the uncertainties of the velocity.

The results indicate that the velocities of atomic hydrogen and helium are the same, suggesting that in the present device, the velocity of any single species, as measured in the vicinity of the exit plane, closely represents the mean mass velocity (within the uncertainty of the measurement). This conclusion is significant because it implies that species specific velocity-measurement techniques such as LIF need only be applied to a single species. In a hydrogen arcjet, it is much easier to probe the atomic hydrogen than the molecular hydrogen, furthermore, it is often easier to probe electronic excited states.

For further investigation of the effect of collisions, it would be interesting to extend these slip measurements further along the axis of the plume to see where slip develops. This extention, however, would require a test chamber capable of maintaining high vacuum

back pressures that would better reproduce the thruster plume structures expected in flight conditions.

Acknowledgments

This work was supported by NASA Lewis Research Center with F. M. Curran as technical monitor. We are grateful to NASA for supplying the arcjet and power processing unit.

References

[1]Miller, D. R., "Free Jet Sources," *Atomic and Molecular Beam Methods Volume 1*, edited by G. Scoles, Oxford Univ. Press, New York, 1988, pp. 41–44.

[2]Mitra, N. K., and Fiebig, M., "Flow in a Laval Nozzle with Gas Mixtures of Disparate Molecular Masses," in *Rarefied Gas Dynamics Volume II*, edited by H. Oguchi, Univ. of Tokyo Press, 1984, pp. 655–664.

[3]Welle, R. P., Pollard, J. E., Janson, S. W., and Cohen, R. B., "One Kilowatt Hydrogen and Helium Arcjet Performance," AIAA Paper 91-2229, June 1991.

[4]Liebeskind, J. G., Hanson, R. K., and Cappelli, M. A., "Laser-Induced Fluorescence Diagnostic for Temperature and Velocity Measurements in a Hydrogen Arcjet Plume," *Applied Optics*, Vol. 32, No. 30, 1993, pp. 6117–6127.

[5]Liebeskind, J. G., Hanson, R. K., and Cappelli, M. A., "Plume Characteristics of an Arcjet Thruster," AIAA Paper 93-2530, June 1993.

[6]Chapman, S., and Cowling, T. G., *The Mathematical Theory of Non-Uniform Gases*, Cambridge Univ. Press, New York, 1970, Chap. 8, pp. 134–150.

[7]Mitra, N. K., Fiebig, M., and Schwan, W., "Quasi-One-Dimensional Nozzle Flows of Disparate Mixtures," *Physics of Fluids*, Vol. 27, No. 10, 1984, pp. 2424–2428.

[8]Curran, F. M., and Haag, T. W., "An Extended Life and Performance Test of a Low Power Arcjet," AIAA Paper 88-3106, July 1988.

[9]Curran, F. M., Bullock, S. R., Haag, T. W., Sarmiento, C. J., and Sankovic, J. M., "Medium Power Hydrogen Arcjet Operation," AIAA Paper 91-2227, June 1991.

[10]Manzella, D. H., Curran, F. M., Myers, R. M., and Zube, D. M., "Preliminary Plume Characteristics of an Arcjet Thruster," AIAA Paper 90-2645, July 1990.

[11]Crofton, M. W., Welle, R. P., Janson, S. W., and Cohen, R. B., "Temperature, Velocity and Density Studies in the 1 kW Ammonia Arcjet Plume by LIF," AIAA Paper 92-3241, July 1992.

[12]Cappelli, M. A., Liebeskind, J. G., Hanson, R. K., Butler, G. W., and King, D. Q., "A Direct Comparison of Hydrogen Arcjet Thruster Properties to Model Predictions," 23rd International Electric Propulsion Conf., IEPC-93-220, Sept. 1994.

Direct Coupling of Euler Flow Equations with Plate Finite Element Structures

Guru P. Guruswamy* and Chansup Byun†
NASA Ames Research Center,
Moffett Field, California 94035

Introduction

In recent years, significant advances have been made for single disciplines in both computational fluid dynamics (CFD) using finite difference approaches[1] and computational structural dynamics (CSD) using finite element methods (see Chap. I of Ref. 2). For aerospace vehicles, structures are dominated by internal discontinuous members such as spars, ribs, panels, and bulkheads. The finite element (FE) method, which is fundamentally based on discretization, has proven to be computationally efficient to solve aerospace structures problems. The external aerodynamics of aerospace vehicles is dominated by field discontinuities such as shock waves and flow separations. Finite difference (FD) computational methods have proven to be efficient to solve such problems.

Problems in aeroelasticity associated with nonlinear systems have been solved using both uncoupled and coupled methods.[3] Uncoupled methods are less expensive but are limited to very small perturbations with moderate nonlinearity. However, aeroelastic problems of aerospace vehicles are often dominated by large structural deformations and high-flow nonlinearities. Fully coupled procedures are required to solve such aeroelastic problems accurately.

In computing aeroelasticity with coupled procedures, one needs to deal with fluid equations in an Eulerian reference system and structural equations in a Lagrangian system. Also, the structural system is physically much stiffer than the fluid system. As a result, the numerical matrices associated with structures are orders of magnitude stiffer than those associated with fluids. Therefore, it is numerically inefficient or even impossible to solve both systems using a single system of equations. To solve this problem, Guruswamy and Yang[3] presented a numerically accurate and efficient approach for two-dimensional airfoils by independently modeling fluids using FD-based transonic small perturbation (TSP) equations and structures using modal equations and coupling the solutions only at boundary interfaces between fluids and structures. This approach has been extended for more complete flow equations on the Euler/Navier-Stokes equations.[4] The modal approach significantly reduces the number of structural unknowns to a great extent when compared to a direct use of FE equations. However, a detailed FE model is required to generate modal data particularly in the absence of experimentally measured data. One can take direct advantage of available FE data and directly couple them with flow equations. By directly using FE data, the possible errors caused by modal approximations can be avoided, and detailed results such as stresses can be computed directly.

In this work, a procedure to compute aeroelasticity by directly coupling the Euler equations for fluids and with plate finite element equations for structures is presented. The coupled equations are solved using a time-integration method. The time accuracy is maintained using moving grids that conform to aeroelastically deformed shape computed every time step. The aerodynamic forces are transferred to structures by using simple lumped load (LL) approach and also a more accurate virtual surface (VS) approach. The VS approach developed in this work can preserve the work done by aerodynamic forces due to structural deformations. The VS approach is validated by computing the aeroelastic response of a wing and comparing with experiment. All aeroelastic responses are computed at transonic Mach numbers where strong coupling between fluids and structures is required.

Fluid-Structural Interfaces

The finite element matrix form of the aeroelastic equations of motion can be written as

$$[M]\{\ddot{q}\} + [G]\{\dot{q}\} + [K]\{q\} = \{Z\} \tag{1}$$

where $[M]$, $[G]$, and $[K]$ are the global mass, damping, and stiffness matrices, respectively. $\{Z\}$ is the aerodynamic force vector corresponding to the nodal displacement vector $\{q\}$. The aerodynamic force vector $\{Z\}$ is computed by solving Euler flow equations using ENSAERO. The plate option of the ANS4 shell/plate element is used to represent the structural properties of the wing configuration.[5]

The main effort after selecting the FE model of the structure falls into computing the global force vector $\{Z\}$ of Eq. (1). $\{Z\}$ is computed by solving the Euler equations at given time t. First, the pressures are computed at all surface grid points. The forces corresponding to the nodal DOF are computed using the fluid-structural interfaces discussed in the following section.

In aeroelastic analysis, it is necessary to represent equivalent aerodynamic loads at the structural nodal points and to represent de-

Presented as Paper 93-3087 at the AIAA 24th Fluid Dynamics Conference, Orlando, FL, July 6–9, 1993; received July 26, 1993; revision received April 7, 1994; accepted for publication April 7, 1994. Copyright © 1994 by the American Institute of Aeronautics and Astronautics, Inc. No copyright is asserted in the United States under Title 17, U.S. Code. The U.S. Government has a royalty-free license to exercise all rights under the copyright claimed herein for Governmental purposes. All other rights are reserved by the copyright owner.

*Research Scientist, Computational Aerosciences Branch. Associate Fellow AIAA.

†Research Scientist, MCAT Institute, Computational Aerosciences Branch. Member AIAA.